Multi-Channel Single-Mode Polymer Waveguide Fabricated Using the Mosquito Method

Sho Yakabe , Hitomi Matsui, Yui Kobayashi, Yuki Saito, Ken Manabe, and Takaaki Ishigure , *Senior Member, IEEE*

Abstract—We experimentally demonstrate that the Mosquito method is capable of fabricating polymer optical waveguides with single-mode cores. The Mosquito method we developed is a technique to form planar polymer waveguides using a commercially available microdispenser. In this article, the flow of the core monomer dispensed from the tip of the needle is simulated using fluid analysis software. The results show that the shape of the needle periphery significantly affects the fabrication of perfectly circular cross-sectional cores. In addition, we demonstrate that the Mosquito method is capable of reducing the MFD variation to 0.4 μm. We find such a small MFD fluctuation is comparable to that of typical single-mode optical fibers.

Index Terms—Mosquito method, polymer optical waveguide, single-mode waveguide, 3-D fluid analysis.

I. INTRODUCTION

IN RECENT years, with the rapid development of cloud computing services, large-scale data centers need to increase the processing speed of switches and servers while reducing power consumption. A promising technology for sustaining the growth of datacenter network capacity is optical interconnections using optical fibers as transmission lines. Optical cables with local connectors (LC connectors) on both ends (for single or duplex cables) have been widely deployed to connect racks in data centers, but those cables are gradually replaced by fiber ribbons with multiple-fiber push-on (MPO) connectors to increase the bandwidth density at board edges. In recent years, even the number of fibers to be aligned in an MPO connector has increased to realize higher bandwidth density [1]. Hence, introduction of multicore fibers (MCFs) is expected as a solution to dramatically increase the number of optical channels per connector cross-sectional area. Some optical connectors have been reported that improve the optical channel per cross-sectional area several times or more by replacing existing single-core fibers (SCFs) with MCFs [2]. However, there are several important issues in introducing MCFs into datacenter networks. For instance, since semiconductor lasers are generally aligned inline (one dimension) in optical transceivers, a fan-in/fan-out (FIFO) device is necessary to couple MCFs to the transmitters and receivers, which need to convert the core alignment in a 1D array to a 2D hexagonal array in MCFs. Various techniques have been proposed as FIFO methods [3], [4]. In particular, a three-dimensional waveguide can realize a small size and low connection loss FIFO device [5].

Meanwhile, we have reported the "Mosquito method" to fabricate polymer waveguides with 2D and 3D multiple core alignment using a microdispenser in order to apply the waveguides to on-board optical interconnects [6]–[8].

Therefore, in this paper, we fabricate single-mode waveguides with multiple circular cores that show small fluctuations of mode-field diameter (MFD) and intercore pitch from the desired values, in order to create a unique FIFO device.

II. THE MOSQUITO METHOD

Generally, single-mode waveguides have been fabricated applying various methods such as photolithography using photomasks [9], [10], UV imprinting [11], and direct curing lithography [12], [13]. When using a photomask, although the core pitch conversion and the core crossing structures can be easily designed, the patterns are formed just on one plane. Furthermore, since the formed core shape is rectangular, when the waveguide is connected to single-mode fibers (SMF) with a circular core, the mode field mismatch causes connection losses.

On the other hand, we have reported the Mosquito method to fabricate polymer waveguides using a microdispenser and a multi-axis syringe scanning robot. The waveguide fabrication procedure in the Mosquito method is schematically shown in Fig. 1. First, a liquid cladding monomer is cast on an organic substrate (mold) formed by injection molding, as shown in Fig. 1(a). Here, the material of the mold is polyphenylene sulfide doped with glass filler, which is the same material as the mechanical transfer (MT) ferrule. We use an MT ferrule based substrate to investigate the possibility of directly forming the waveguide in an MT ferrule, which would connect with an SMF array terminated with other MT connectors. We already succeeded in fabricating

Sho Yakabe is with the Graduate School of Science and Technology, Keio University, Yokohama 223-8522, Japan, and also with the Sumitomo Electric Industries Ltd., Yokohama 244-8588, Japan (e-mail: yakabe-syou@sei.co.jp).

Hitomi Matsui and Yui Kobayashi are with the Graduate School of Science and Technology, Keio University, Yokohama 223-8522, Japan (e-mail: matsui-hitomi@z8.keio.jp; pi-0bses_1iibelve7@z3.keio.jp).

Yuki Saito and Ken Manabe are with the Sumitomo Electric Industries Ltd., Yokohama 244-8588, Japan (e-mail: manabe-ken@sei.co.jp; saito-yuki@sei.co.jp).

Takaaki Ishigure is with the Faculty of Science and Technology, Keio University, Yokohama 223-8522, Japan (e-mail: ishigure@appi.keio.ac.jp).

Color versions of one or more of the figures in this article are available online at https://ieeexplore.ieee.org.

Digital Object Identifier 10.1109/JLT.2020.3029395
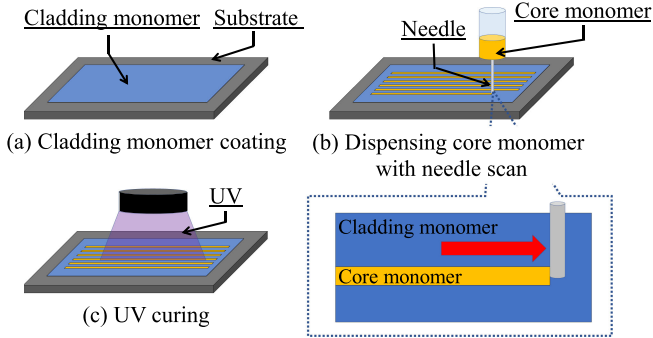
Fig. 1.   Procedure of polymer waveguide fabrication by the Mosquito method.

Fig. 2.   Schematic diagram of core monomer dispense in cladding monomer in the Mosquito method.

a multimode polymer waveguide in a polymer waveguide MT (PMT) connector using the Mosquito method [14] and tried to connect the waveguide with multimode fiber ribbons with an MT connector. Because of the multimode waveguide's large core diameter, the required core position accuracy is moderate. So, the guide pins on the MT connector are good enough to attain high coupling efficiency. Contrastingly, in the connection between two single-mode cores in an MT connector, a radial offset (even due to the thermal expansion of the waveguide or connector materials) could cause connection loss, so it is a good design decision for the ferrule and the substrate to be made of the same material. Furthermore, in order to cast the cladding monomer with a uniform thickness on the substrate, a microdispenser is used even to dispense the cladding monomer, the temperature of which is precisely controlled. After casting the cladding monomer, the tip of a thin needle attached to a syringe is inserted into the cladding monomer (as shown in the inset of Fig. 1(b)), and the core monomer is dispensed into the cladding monomer while the needle scans following the programmed core patterns, as shown in Fig. 1(b). In order to form multiple cores, the needle scan is repeated to align the multiple cores. After all the cores are dispensed, both the core and cladding monomers are cured under UV light, as shown in Fig. 1(c).

In the Mosquito method, it is possible to three-dimensionally align the cores by scanning the needle in the direction perpendicular to the substrate using the multi-axis syringe-scan robot. Furthermore, since the core cross-sectional shape of the waveguide fabricated using the Mosquito method is circular, the waveguide is suitable to connect with SMFs because the mode fields can more easily match.

III. Core Diameter Design for Single-Mode Operation

In order to fabricate single-mode waveguides using the Mosquito method, the dispensing conditions are investigated as follows: Since the waveguide fabricated using the Mosquito method has a circular core cross-sectional shape, the single-mode condition is simply calculated by applying the same equation as that for optical fibers with a circular core expressed in equation (1).

In this paper, silicate-based organic-inorganic hybrid resins are utilized. The refractive indices of the core and cladding
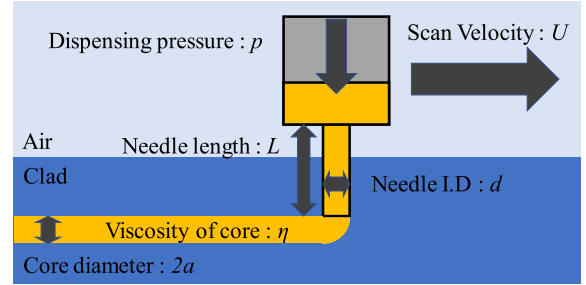
polymers at 1.31 μm are 1.577 and 1.568, respectively. The relative index difference (Δ) and numerical aperture (NA) are calculated to be 1.9% and 0.168, respectively.

$$V = \frac{2\pi a}{\lambda} NA \qquad (1)$$

Here, V represents the normalized frequency, a represents the core radius, and λ represents the free-space wavelength. When the circular core in an optical fiber has a step-index (SI) profile in it, it is well known that V smaller than 2.405 needs to be satisfied to support just one LP mode in the core. Since the NA is fixed when the core and cladding materials are determined, while the operating wavelength is 1.31 μm or longer, the core radius is the only parameter which can be adjusted to make the fabricated waveguides satisfy the single-mode condition. The calculated core radius to satisfy the single-mode condition is smaller than 3 μm.

Furthermore, in order to fabricate such a small core, we investigate the dispensing condition of the core monomer from a thin needle. The monomer flow rate Q is analytically derived by the Navier–Stokes equation described by equation (2). Here, the initial diameter $2a$ of the dispensed core monomer is described by equation (3), from which the fabricated core diameter can be predicted.

$$Q = \frac{\pi d^4 p}{128 \eta L} \qquad (2)$$

$$2a = 2\sqrt{\frac{Q}{\pi U}} = \sqrt{\frac{p d^4}{32 L \eta U}} \qquad (3)$$

Here, p represents the dispensing pressure, L represents the needle length, d represents the needle inner diameter (I.D.), η represents the monomer viscosity, and U represents the needle-scan velocity. Fig. 2 shows a schematic diagram of core monomer dispensing by scanning the needle in the cladding monomer. Waveguides are fabricated under the fabrication conditions shown in Table I, under which the initial core diameter to be dispensed is calculated to be 4.1 μm, which is smaller than the maximum core diameter of 6 μm calculated to satisfy the single-mode condition. Fig. 3 shows an entire cross-section of a fabricated waveguide and Fig. 4 shows zoomed-in cross-sections of some cores in the waveguide shown in Fig. 3. Meanwhile, Fig. 5 shows the near-field patterns (NFPs) from the same cores

TABLE I
FABRICATION CONDITIONS FOR SINGLE-MODE POLYMER WAVEGUIDES

Dispensing pressure : p	500 kPa
Needle length : L	15 mm
Needle I.D : d	100 μm
Viscosity of core : η	76,000 cP
Scan Velocity : U	80 mm/sec
Core diameter : $2a$	4.1 μm

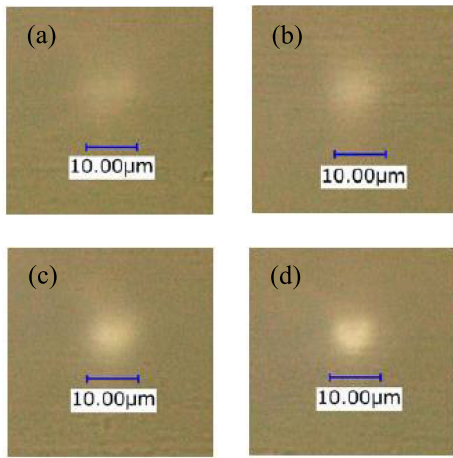Fig. 3. Entire cross-section of a fabricated single-mode polymer waveguide.

Fig. 4. Cross-section of some cores in the waveguide shown in Fig. 3 (a) Ch.2 (b) Ch.5 (c) Ch.8 (d) Ch.12.

Fig. 5. NFP at a wavelength of 1.31 μm from some cores in the waveguide shown in Fig. 3 (a) Ch.2 (b) Ch.5 (c) Ch.8 (d) Ch.12.

shown in Fig. 4. The core is dispensed in order from Ch.1 to Ch.12. The large-size core shown on the far-left side of the cross-section in Fig. 3 is a dummy core with an approximately 50-μm diameter; it is used to align (in particular the core height) the small cores next to the dummy core when we couple the waveguide cores to an SMF just by first roughly aligning the SMF to the large core.

From the cross-sections of the polymer waveguide shown in Figs. 3 and 4, we find that circular cores with a core diameter of 10 μm or less are successfully formed. However, we also confirm that the boundary between the core and cladding is not clear, particularly in the lower channel numbers. Hence, the core diameter is not necessarily measured accurately from the observed image of the cross-section. It is also confirmed by the NFP measurement at a wavelength of 1.31 μm, shown in Fig. 5, that all the cores satisfy the single-mode condition. Here, the propagating modes in the waveguide core are launched using a 1-m long SMF probe (A typical SMF compliant to ITU-T G. 657. A1, with an MFD of 8.6 ± 0.4 μm at 1.31 μm) to measure the NFP.

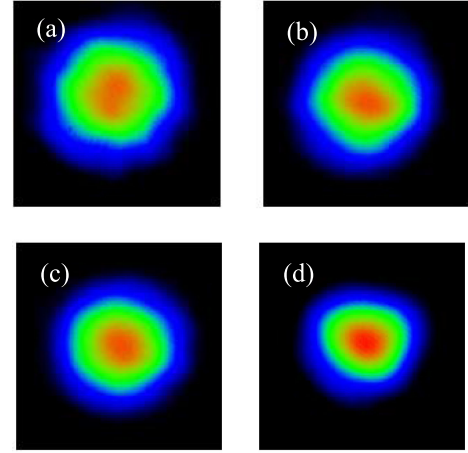The observed intensity profiles fit a Gaussian profile featuring LP_{01} mode. After confirming the LP_{01} mode is launched, the SMF probe is slightly misaligned in the radial direction from the core center, and then existence of the other intensity peaks featuring higher order modes are examined. No intensity peaks for the higher order modes indicates single-mode operation in the corresponding core. Thus, it is exhibited that the Mosquito method is possible to fabricate circular core single-mode waveguides by applying the fabrication conditions derived theoretically.

On the other hand, in order to apply this single-mode waveguide to an optical component with functions of pitch conversion and connection with an SMF array (e.g., FIFO devices for MCFs), there are several issues to be addressed. One is the MFD uniformity: the MFD measured in the horizontal (X-axis, MFD(X)) and the vertical (Y-axis, MFD(Y)) directions shown in Fig. 5 are slightly different. This difference in the MFDs measured in the two orthogonal directions means that the mode-field has an elliptic profile. Another issue is the MFD variation among the multiple cores dispensed in one waveguide. In the Mosquito method, each core is dispensed serially, and after all the cores are dispensed, both the core and cladding monomers are simultaneously exposed to UV light for curing. Hence, an "interim time," which is defined as the time from when one core monomer is just dispensed to when the UV curing starts, varies among different channels. During the interim time, the liquid core and cladding monomers diffuse mutually to have concentration distributions in the core, which leads to a graded-index (GI) profile. The GI profile formed in the core affects the MFD, similar to the effect of a lower NA on the MFD. Thus, the MFD variation is caused by the different interim times among the multiple cores. Fig. 6 shows the dependences of MFD(X) and MFD(Y) on the interim time (channel number). Fig. 6 also shows the MFD ratio (MFD(X)/MFD(Y)), which is a measure of the circularity of the mode field. It is found from Fig. 6 that the mode field is horizontally long elliptic for shorter interim times (larger channel numbers). However, with increasing the interim time (smaller channel number), the MFD ratio approaches 100%, which indicates a perfect circle.
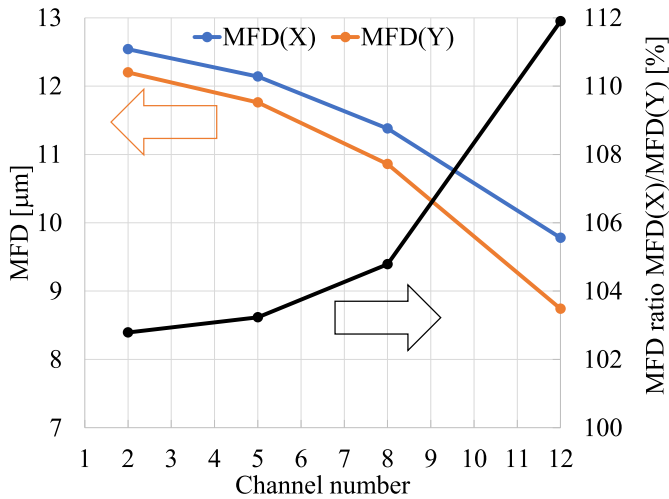
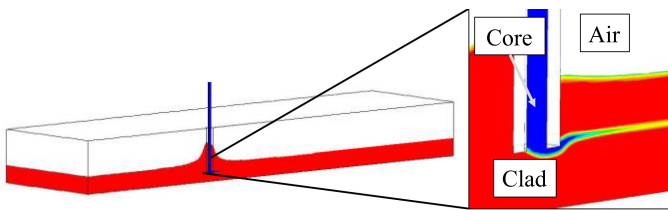Fig. 6.   MFD ratio from some cores in the waveguide.

Fig. 7.   Flow analysis model for the Mosquito method.

TABLE II
PARAMETERS OF THE MONOMER USED FOR THE FLUID ANALYSIS

	Core monomer	Cladding monomer
Viscosity	71 Pa·s	3.47 Pa·s
Surface tension		31.1 mN/m
Density	1.20 g/ml	1.17 g/ml

IV. CIRCULARIZATION OF CORE SHAPE

The core shape and mode field of typical SMFs are circular. Hence, there is a concern that fabricated polymer waveguides exhibiting elliptic mode fields (MFD variation) could increase the connection loss due to the MFD mismatch when connecting to SMFs. Therefore, in order to form circular cores, the flow of the core monomer after being dispensed from the needle tip into the cladding monomer is theoretically simulated using flow analysis software. Here, the general-purpose thermal fluid analysis software *ANSYS Fluent* is used for the analyses. Fig. 7 shows the flow analysis model for the Mosquito method. This model is composed of two layers of fluid, the cladding monomer and the air in addition to the dispensed core monomer. For the monomer flow calculation, three parameters of the two monomers are taken into account: viscosity, surface tension, and density; they are summarized in Table II.

Fig. 8 shows a side view cross-section of the core monomer dispensing, where the broken lines (a), (b) and (c) are the positions of the needle center, the needle back-side edge, and
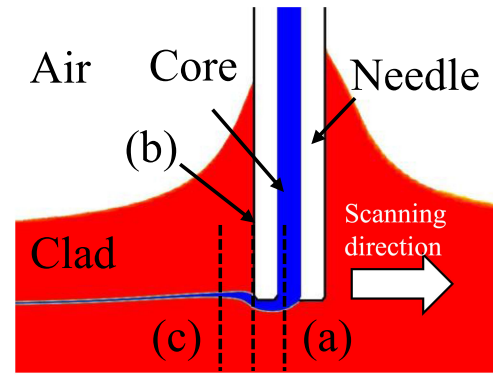

Fig. 8.   Side view cross-section of the core monomer flow in the fluidic simulation: broken line (a) center of the needle (b) back-side needle edge (c) 0.1 mm behind the needle.
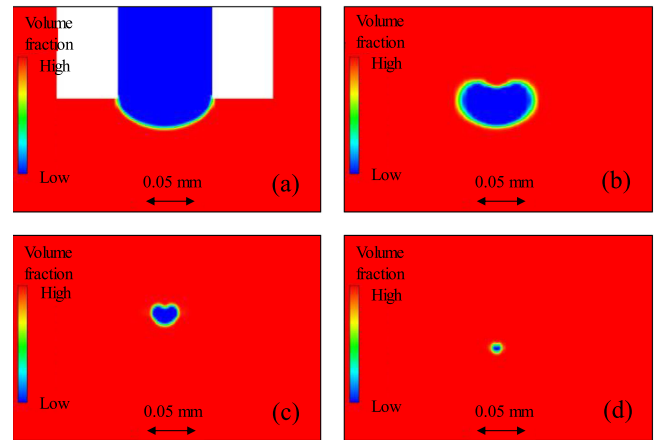

Fig. 9.   Cross-sections perpendicular to the needle-scan direction during the core monomer dispense (a) center of the needle (b) back-side needle edge (c) 0.1 mm behind the needle (d) 9 mm behind the needle.

0.1 mm behind the needle back-side edge, respectively. Meanwhile, Fig. 9 shows cross-sections perpendicular to the needle scan direction, where the four cross-sections include the each broken line shown in Fig. 8 in addition to a plane 9 mm behind the needle back-side edge.

We already simulated the side view cross-section using the *COMSOL Multiphysics* software in the same way [15], and showed that just after being dispensed, the core monomer ascends slightly in the cladding monomer and gradually descends after leaving the needle. The core monomer flow trajectory shown in Fig. 8 shows good agreement with our previously calculated and measured results. It should be noted that a triangle shape on the top of the cladding monomer creeping up around the needle surface is accurately simulated in Fig. 8 by taking the surface tension and the layer of the air above the cladding monomer into consideration.

It is also noteworthy that the core monomer cross-sectional shape perpendicular to the needle-scan direction can be calculated in this simulation tool as shown in Fig. 9. From Fig. 9, we find that the core monomer cross-sectional shape just after being dispensed is not a circle but is a horizontally long ellipse with a
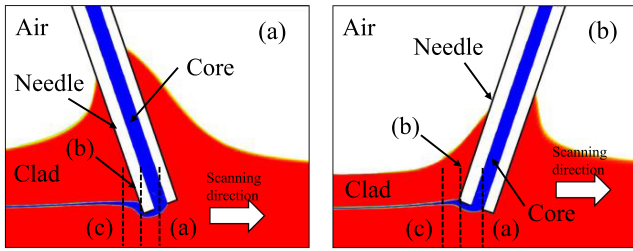
Fig. 10. Side view cross-sections of the monomer flow under tilted dispensed angles (a) +20 ° (b) −20 °.
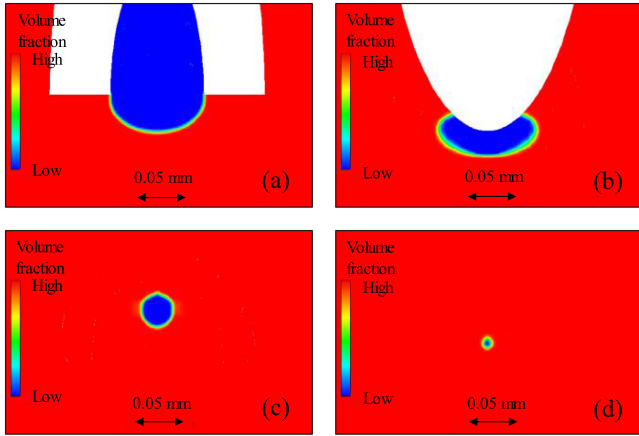

Fig. 11. Cross-sections perpendicular to the needle-scan direction during the core monomer dispense under tilted dispensed angle of +20° (a) center of the needle (b) back-side needle edge (c) 0.1 mm behind the needle (d) 9 mm behind the needle.
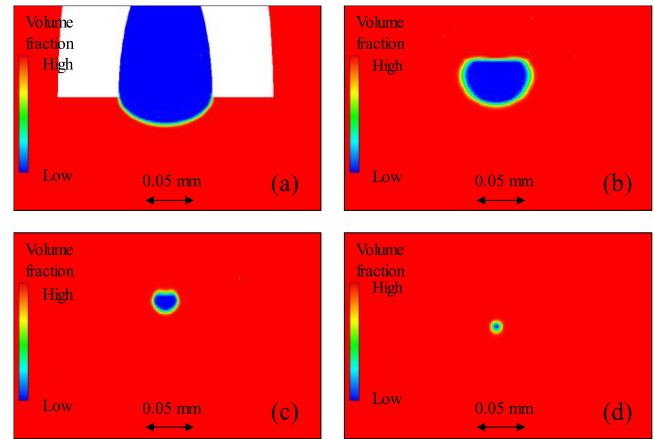

Fig. 12. Cross-sections perpendicular to the needle-scan direction during the core monomer dispense under tilted dispensed angle of −20° (a) center of the needle (b) back-side needle edge (c) 0.1 mm behind the needle (d) 9 mm behind the needle.

small dip on the top. So, a heart-like shape is observed in Figs. 9 (b) and (c). However, the dip on the top gradually disappears as it leaves the needle, while the elliptic shape is preserved even if the core size decreases to approximately 10 μm or less, as shown in Fig. 9(d). The experimentally observed cross-section shown in Fig. 4(d) has a horizontally long elliptic shape with a dip on the top, which well agrees with the calculated cross-sectional shape.

In order to form a core with a circular shape, the relationship between the core monomer flow and the dispensing direction is investigated. The dispensing direction we have employed has been perpendicular to the scanning direction and perpendicular to the substrate surface, as shown in Figs 1, 2. 7, and 8. On the other hand, as shown in Fig. 10, in this paper, the dispensing direction is tilted with an angle of 20° with respect to the original dispensing direction (the original direction is defined as 0°). When the needle tip is inclined to the scanning direction, the dispensing angle is defined to be positive, so the dispensing angles shown in Figs. 10(a) and (b) are +20° and −20°, respectively. Under these conditions, the cross-sectional shapes of the core monomer are calculated in the same way as those in Figs. 8 and 9. Fig. 10 show the side view cross-sections under the tilted dispensing angles. Figs. 11 and 12 show cross-sections perpendicular to the scan direction: the same planes as those in Fig. 9 when the needle is tilted with angles of +20° and –20°, respectively.

From Figs. 11 and 12, the cross-sections of the core monomer at a position 0.1 mm behind the needle back-side edge is different from when the needle is perpendicular to the scanning direction (0° dispensing angle). In particular, at a needle inclination of +20°, the cross-sectional shape of the core monomer is circular. From this result, in order to fabricate circular cores by the Mosquito method, it is effective to incline the needle.

However, angling the needle restricts the scanning direction, so it is not appropriate to form a three-dimensional waveguide structure. From the calculated results, we find that the core cross-sectional shape just after being dispensed is largely affected by the ascension of the core monomer at the back-side edge of the needle. When the dispensing angle is 0°, the edge of the needle scrapes a dip into the top of the core area. After the core monomer exits the back-side edge, it ascends along the edge of the needle because a lower pressure area exists just behind the needle [15]. However, the core monomer does not sufficiently ascend to fill the dip and thus, a heart-like shape remains. On the other hand, if the needle is angled to +20°, the core monomer ascends enough to fill the dip. We find from the simulation that the needle outer-wall declination is a key to let the core monomer ascend higher. Therefore, we investigate whether a tapered needle with a declined outer wall can work as well as an angled needle. The taper angle (outer wall angle) of this needle is measured to be about 10°.

Fig. 13 shows cross-sections of some cores in the fabricated waveguide and Fig. 14 shows the NFP from the same cores shown in Fig. 13. From Figs 13 and 14, it can be seen that the cores are formed with an almost perfect circular cross-sectional shape. Furthermore, the MFDs and the MFD ratio (MFD(X)/MFD(Y)), which is a measure of the circularity of the mode field are shown in Fig. 15. The results in Fig. 15 show that the MFD ratio stays within a 10% deviation from 100% among all the cores, and there is no channel dependence. Compared to the results in Fig. 6, the circularity of the cores could increase by applying a tapered needle.

In addition, the core geometry is analyzed by fluid simulation. Fig. 16 shows the side view cross-section of monomer flow using
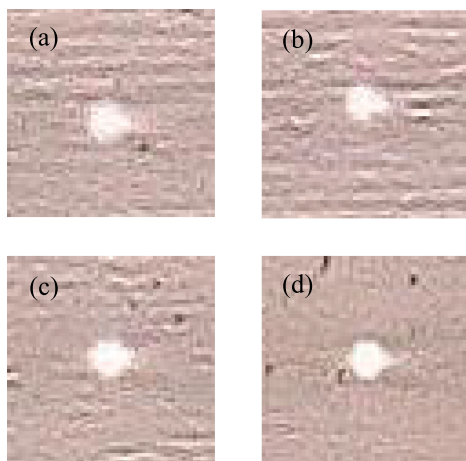
Fig. 13. Cross-section of some cores in the waveguide. (a) Ch.2 (b) Ch.5 (c) Ch.8 (d) Ch.10.
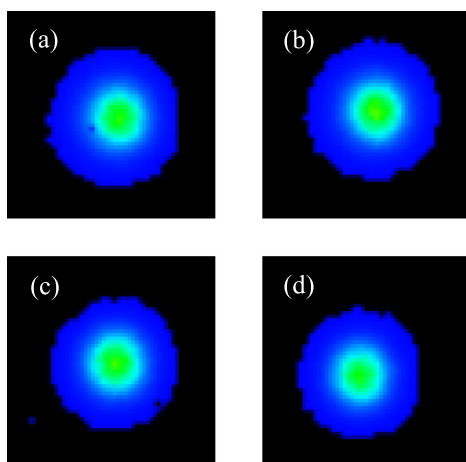

Fig. 14. NFP from some cores in the waveguide shown in Fig. 14 (a) Ch.2 (b) Ch.5 (c) Ch.8 (d) Ch.10.
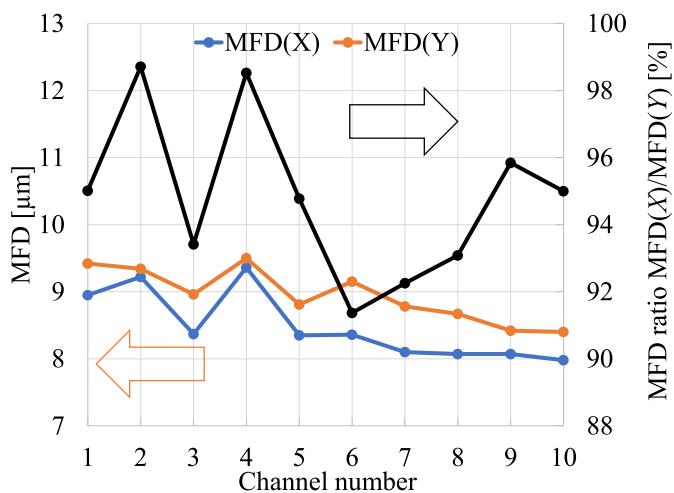

Fig. 15. MFD and MFD ratio of each cores in the waveguide.
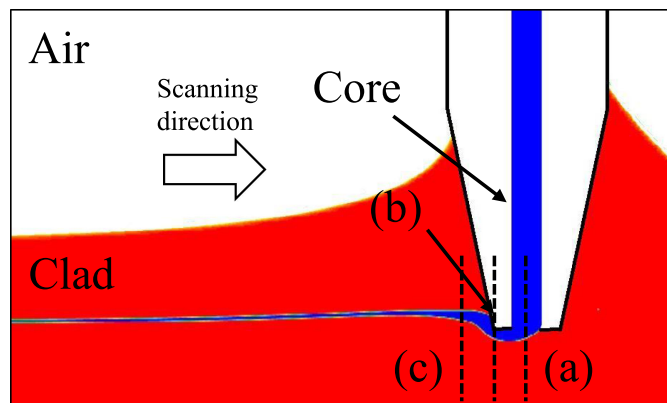

Fig. 16. Side-view cross-section of the core monomer flow in the fluidic simulation: broken line (a) center of the needle (b) back-side needle edge (c) 0.1 mm behind the needle.
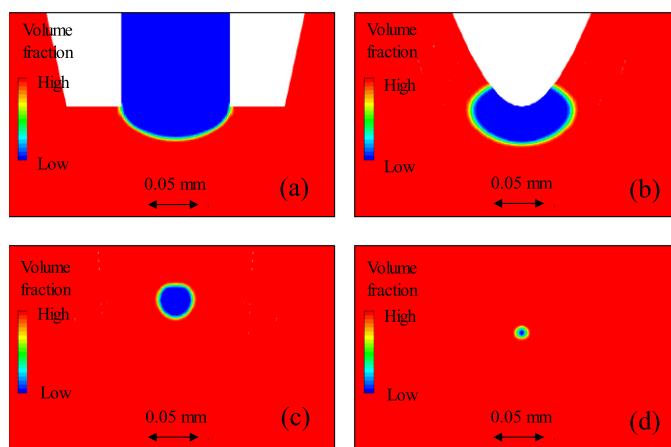

Fig. 17. Cross-sections perpendicular to the needle-scan direction during the core monomer dispense with tapered needle (a) center of the needle (b) back-side needle edge (c) 0.1 mm behind the needle (d) 9 mm behind the needle.

a tapered needle. Fig. 17 shows cross-sections perpendicular to the scan direction. The shape of the core monomer at each position in Fig. 17 is found to be very similar to the shapes in Figs. 11 and 13.

The experimental and analytical results show that a more circular core shape can be formed using the Mosquito method by optimizing the shape of the needle.

V. MFD STABILIZATION AMONG MULTIPLE CORES

The MFD uniformity among the multiple cores is also a very key issue to connect the waveguide to an SMF array with low loss. The SMF used for the waveguide evaluation in this paper is compliant to ITU-T G. 657. A1, to have an MFD of 8.6 $\pm$ 0.4 μm at a wavelength of 1.31 μm. Hence, we want the MFDs of the multiple cores in the single-mode waveguide to be uniform and identical to that of the SMF. As shown in Figs. 3 and 4, the boundaries between the core and the cladding are unclear, particularly for the cores with a long interim time, due to the mutual diffusion between the core and cladding monomers. Furthermore, since this mutual diffusion between
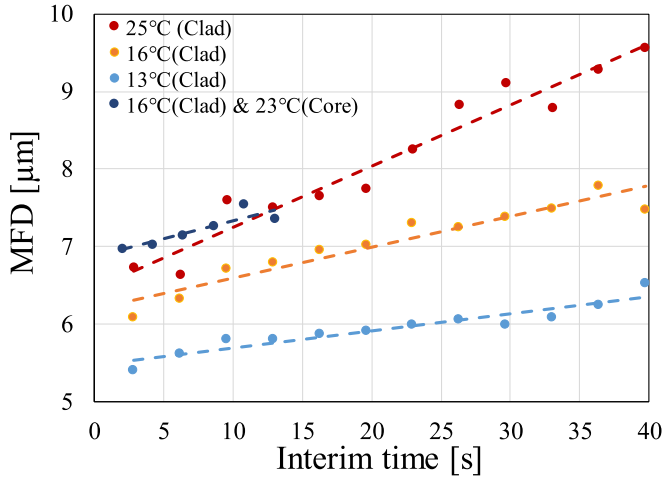
Fig. 18. Relationship between interim time and MFD of the waveguides fabricated under different cladding monomer temperature.
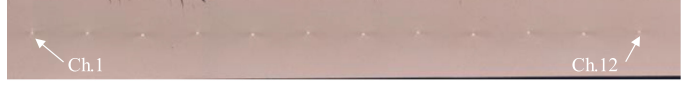

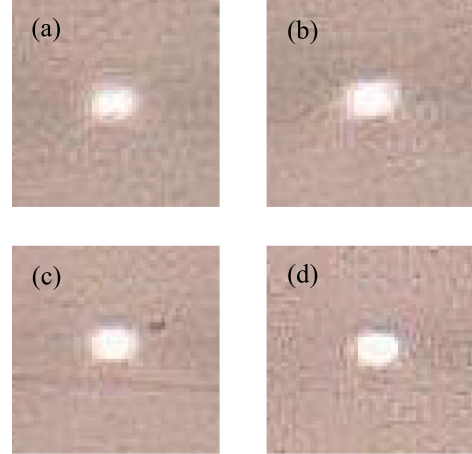Fig. 19. Cross section of a single-mode polymer waveguide fabricated under controlled monomer temperature.

Fig. 20. Cross-sections of some cores in the fabricated waveguide under controlled temperature (a) Ch.2 (b) Ch.5 (c) Ch.8 (d) Ch.12.

the core and cladding monomers reduces the refractive index difference between the core and cladding, the light confinement in the core weakens, and then the MFD increases due to the larger evanescent field. From Figs. 5 and 6, we actually find that the MFD increases with increasing the interim time, which could be due to both the actual core area increment and NA decrement. If we suppose no monomer diffusion (an SI profile is formed), the NA of the waveguides composed of the polymers used in this paper is calculated to be 0.168. Applying this NA value to the *V*-parameter in eq. (1), the MFD of the core with a diameter of 4 μm is calculated to be 6.4 μm by eq. (4) [16]. However, the measured MFD of Ch. 12 to which even the shortest interim time is applied is larger than 8 μm. So, in order to form the multiple cores with a uniform MFD, the monomer diffusion should be controlled.

$$MFD = 2a \left(0.65 + \frac{1.619}{V^{3/2}} + \frac{2.879}{V^6} \right) \quad (4)$$

In this paper, we focus on the temperature of the monomers in order to control the mutual diffusion. In steps (a) and (b) of the Mosquito method shown in Fig. 1, the temperature of the cladding monomer on a substrate is kept lower than room temperature (23 °C) by placing the substrate with the cladding monomer on a Peltier plate. From step (a) to (b), the core is formed after the temperature of the cladding monomer stabilizes. Then, the MFD of the fabricated waveguides under different monomer temperature is measured at a wavelength of 1.31 μm by an NFP camera, similar to those shown in Fig. 5. Fig. 18 shows the relationship between the interim time and the MFD under different temperatures, 13 °C, 16 °C and 25 °C. Furthermore, the results of the waveguide under controlled temperatures for both the cladding and core monomers are also presented.

From the result shown in Fig. 18, it is obvious that the mutual diffusion between the core and cladding monomers is controlled by keeping the monomer temperature low; the MFD of the cores formed at 25 °C is larger than those at 13 °C with the same interim time. In addition, the MFD shows lower dependence on the interim time by keeping the monomer at a low temperature. When the temperature of the monomer is 25 °C, the slope of the MFD with respect to the interim time in Fig. 18 is approximated to 0.08 μm/s, while at 13 °C the MFD slope decreases to one fourth (0.02 μm/s). As mentioned earlier, the MFD is a measure of the optical confinement in the core: the MFD could increase due not only to a larger core area but also to a lower NA. Therefore, the difference of the MFD slope in Fig. 18 stems from the temperature dependent monomer diffusion rate. It is estimated from the results in Fig. 18 that the maximum difference in MFD (between the channels with the longest and shortest interim times) can be controlled to 0.4 μm or less under low monomer temperature, where the maximum interim time for forming 8 cores with a 10-cm long straight pattern is approximately 10 seconds. As shown in Figs. 19 and 20, the boundary between the core and the cladding is more abrupt in the cross-section of the waveguide fabricated under low monomer temperature, illustrating that the mutual diffusion is controlled. In addition, there is almost no difference among the NFPs in Fig. 21.

Meanwhile, from the cross-section shown in Fig. 19, it is found that the waveguide formed on the polyphenylene sulfide substrate exhibits good adhesion.

On the other hand, Fig. 18 shows that for the core monomer, temperature control has a small effect on the monomer diffusion. When the temperature of only the cladding monomer is kept at 16 °C, the slope of the MFD with respect to the interim time in Fig. 18 is approximately 0.04 μm/s, whereas when the temperature of the core monomer is also controlled at 23 °C to dispense into the cladding at 16 °C, the slope is approximately 0.05 μm/s, showing little change. This could be because the volume of the core monomer dispensed is so small compared to the cladding monomer that the cladding monomer temperature
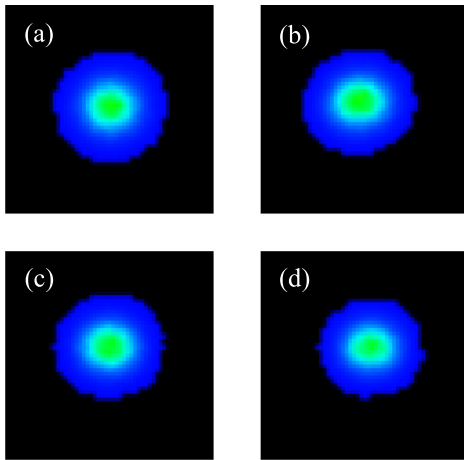
Fig. 21. NFPs of some cores in the fabricated waveguide under controlled temperature (a) Ch.2 (b) Ch.5 (c) Ch.8 (d) Ch.12.
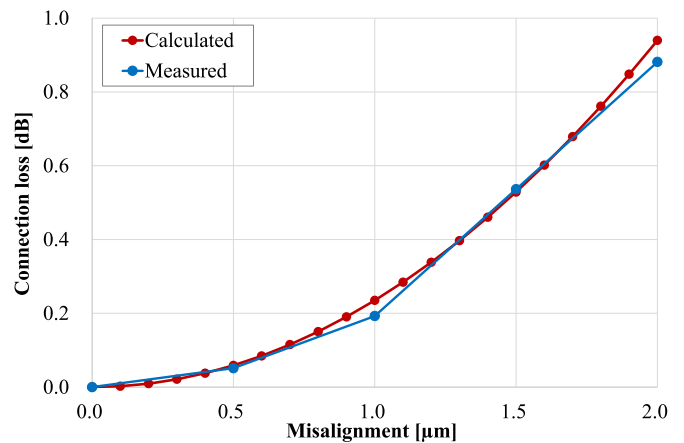

Fig. 22. Measured and calculated connection loss between an SMF and fabricated waveguide with respect to the radial misalignment at the connection point.

dominates. However, controlling the temperature of the core monomer is also important for controlling the MFD variation among multiple waveguide samples. Applying the temperature dependence of the monomer viscosity, it is estimated that a temperature change of 1 °C leads to a change to the core diameter of about 0.7 μm under a fixed dispensing pressure.

The insertion losses of the fabricated 4.5-cm long waveguides are measured at 1.31 μm by butt-coupling to the two SMFs used for the MFD measurement on both of their ends. We find that the insertion losses are between 4.28–4.79 dB and 2.3–3.6 dB among the 12 channels in the waveguides fabricated under 16 °C and 25 °C, respectively. The coupling loss is estimated to 0.6 dB/facet (including 0.4-dB Fresnel loss) in the worst channel by the overlap integral of the NFPs. It is noted that the minimum coupling loss of 0.4 dB/facet (just the Fresnel loss) is observed in all the channels of the waveguide fabricated under 13 °C due to the small MFD fluctuation. Although the MFD fluctuation increases when fabricated under 25 °C due to the monomer diffusion between the core and cladding, such a diffusion contributes to decrease the core-cladding boundary roughness, resulting in low propagation loss. By substituting the coupling losses from the observed insertion loss, the propagation losses of the two waveguides at 1.31 μm are calculated between 0.40–0.53 dB/cm. These values are slightly higher than the values of the potential of this waveguide material: 0.22 dB/cm measured by the cut-back method. Further reduction of the insertion loss of the waveguide will be published elsewhere [17].

VI. IMPROVEMENT IN INTERCORE PITCH ACCURACY

Since the connection loss between two single-mode waveguide cores is very sensitive to core misalignment, a position accuracy of 1 μm or less is required for optical connectors for single-mode waveguides. Similarly, in order to utilize a single-mode waveguide as an optical connection component such as a FIFO device for MCFs, the position accuracy of the core in the waveguides must also be less than 1 μm. Fig. 22 shows a comparison of the theoretical and measured connection losses with respect to a radial misalignment between the SMF and one

channel of the waveguide. Here, the waveguide shown in Fig. 19 is used for the measurement. The calculated loss curve shows the coupling loss due to misalignment when the MFD is assumed to be 8.6 μm at a wavelength of 1.31 μm. Fig. 22 shows that the calculated and measured losses are very close. Although various manufacturing errors could cause misalignment between optical components, we focus only on the core position accuracy, in order to simplify the discussion. In general, misalignment as large as twice the core position accuracy is likely to occur between two MT connectors. Since the connection loss of standard MPO connectors is specified to be 0.75 dB, the core position accuracy in the polymer waveguide should roughly be less than 1 μm from Fig. 22 to satisfy that connection loss specification.

In the waveguides fabricated by the Mosquito method, the intercore pitch accuracy largely depends on the repeatability in positioning of the automatic stage for the needle scan. In commercially available microdispenser systems, a positioning accuracy of ± 5 μm is specified for the built-in automatic stage, so it is impossible to satisfy the required pitch accuracy between cores for single-mode waveguide connections. Therefore, we preliminary improve the intercore pitch accuracy in the fabricated waveguides applying the Mosquito method by utilizing two different automatic stages for scanning the needle.

The first syringe positioning to start dispensing Ch. 1, for which long-distance movement is required, is operated by the automatic stage with low positioning accuracy originally equipped on the robot, while the movement in the Y-axis direction (the parallel core alignment) is operated by the automatic stage with high positioning accuracy. By this two-stage configuration, we realize multiple-core alignment with high position accuracy as well as large dispense area for the Mosquito method. Here, we are able to reproduce positioning within approximately ± 0.5 μm. The intercore pitch in the waveguide fabricated using the two automatic stages are measured from cross-sectional images taken by a microscope. Here, waveguides with a core pitch of 125 μm between 12 cores are fabricated. Then, the standard deviations of the measured intercore pitch is compared. The results of the measurements are shown in Table III. We find

TABLE III
STANDARD DEVIATION COMPARISON OF INTERCORE PITCH

	Standard deviation [μm]
Automatic stage with a low positioning accuracy (The number of measured data is 66.)	2.7
Automatic stage with a high positioning accuracy (The number of measured data is 100.)	1.8

the waveguide fabricated on the stage with a position accuracy of ± 5 μm is calculated to be ± 2.7 μm.

On the other hand, a waveguide fabricated on a high precision automatic stage exhibits an intercore pitch standard deviation of ± 1.8 μm, which represents a 0.9-μm reduction in the standard deviation.

From these results, we experimentally confirm the ability to achieve an intercore pitch accuracy less than 1 μm, as required for single-mode connection. In this paper, we use an automatic stage with a positioning accuracy smaller than 1 μm. Nevertheless, the variation of the core position does not improve significantly: from a standard deviation of 2.7 μm to 1.8 μm. This might originate from the way in which the core position is measured. In this paper, the core position is measured manually in the cross-sectional photo, hence the measurement accuracy should be insufficient to evaluate an accuracy of less than 1 μm.

In the Mosquito method, the core height needs to be precisely controlled (in the vertical direction) as well, in order to efficiently connect to other optical components such as laser/detector and SMF arrays via MT/MPO connectors. We have already reported on the core height control in a *multimode waveguide* [15], and found that the flow of the cladding monomer during needle scan also needed to be taken into consideration to control the core height. Therefore, controlling the core height in *single-mode waveguides* should be a more difficult issue, and it is essential to optimize the fabrication conditions by taking not only the positional accuracy of the automated stage but also the flow of the monomers into account.

VII. CONCLUSION

In order to apply to optical connection components such as FIFO devices for MCFs, we designed polymer optical waveguides with GI circular cores which are fabricated using the Mosquito method to satisfy the single-mode condition, and a method to reduce the fluctuation of the optical characteristics among the multiple cores was investigated both theoretically and experimentally.

In order to fabricate perfectly circular cores, we found from the theoretical fluid analyses that the core monomer flow in the vicinity of the needle tip just after being dispensed was key: the needle back-side edge could form a dip on the cross-section of the core to make a heart cross-sectional shape. In order to address this issue, the needle outer wall on the back-side should

be inclined to the scanning direction. By tilting the outer wall on the back-side of the needle, the dispensed core monomer flows by expanding its flow line vertically, filling in the dip on the top.

Furthermore, keeping the monomer temperature low to control the monomer diffusion between the core and the cladding reduces the variation in MFD among the cores to the same level as the specification of conventional SMFs.

Although it was a concern that fabricating single-mode waveguides using the Mosquito method to exhibit stable characteristics among the multiple cores and a high pitch accuracy required for single-mode core connectors, in this paper we discovered how to address these issues, namely optimization of the fabrication conditions and equipment.

REFERENCES

[1] M. Ohmura, "Highly precise MT ferrule enabling single-mode 32-fiber MPO connector," in *Proc. Int. Wire Cab. Symp.*, 2016, pp. 567–561.

[2] T. Morishima, "MCF-enabled ultra-high-density 256-core MT connector and 96-core physical-contact MPO connector," in *Proc. Opt. Fib. Commun. Conf. Exhbit.*, 2017, Paper Th5D.4.

[3] O. Shimakawa, M. Shiozaki, T. Sano, and A. Inoue, "Pluggable fan-out realizing physical contact and low coupling loss for multi-core fiber," in *Proc. Opt. Fib. Commun. Conf. Exhibit.*, 2013, Paper OM31.2.

[4] H. Arao, O. Shimakawa, M. Harumoto, T. Sano, and A. Inoue, "Compact multi-core fiber fan-in/out using GRIN lens and microlens array," in *Proc. 19th OptoElectron. Commun. Conf.*, 2014, Paper Mo1E-1.

[5] R. R. Thomson *et al.*, "Ultrafast laser inscription of a 3-D fan-out device for multicore fiber coupling applications," in *Proc. Conf. Las. Electro-Opt.*, 2008, Paper JWA62.

[6] K. Soma and T. Ishigure, "Fabrication of a graded-Index circular-core polymer parallel optical waveguide using a microdispenser for a high-density optical printed circuit board," *IEEE J. Sel. Top. Quant. Electron.*, vol. 19, no. 2, Mar./Apr. 2013, Art. no. 3600310.

[7] R. Kinoshita, D. Suganuma, and T. Ishigure, "Accurate interchannel pitch control in graded-index circular-core polymer parallel optical waveguide using the Mosquito method," *Opt. Express*, vol. 22, no. 7, pp. 8426–8437, 2014.

[8] T. Ishigure, D. Suganuma, and K. Soma, "3-D high density channel integration of polymer optical waveguide using the Mosquito method," in *Proc. 64th Electron. Compon. Technol. Conf.*, 2014, pp. 1042–1047.

[9] J. Kobayashi, T. Matsuura, S. Sasaki, and T. Maruno, "Single-mode optical waveguides fabricated from fluorinated polyimides," *Appl. Opt.*, vol. 37, no. 6, pp. 1032–1037, 1998.

[10] M. Nordstrom, D. A. Zauner, A. Boisen, and J. Hubner, "Single-mode waveguides with SU-8 polymer core and cladding for MOEMS applications," *J. Lightw. Technol.*, vol. 25, no. 5, pp. 1284–1289, May 2007.

[11] M. U. Khan *et al.*, "Multi-level single mode 2D polymer waveguide optical interconnects using nano-imprint lithography," *Opt. Express*, vol. 23, no. 11, pp. 14630–14639, 2015.

[12] E. Zgraggen *et al.*, "Laser direct writing of single-mode polysiloxane optical waveguides and devices," *J. Lightw. Technol.*, vol. 32, no. 17, pp. 3016–3042, Sep. 2014.

[13] H. H. Duc Nguyen, U. Hollenbach, U. Ostrzinski, K. Pfeiffer, S. Hengsbach, and J. Mohr, "Freeform 3-D embedded polymer waveguides enabled by external-diffusion assisted two-photon lithography," *Appl. Opt.*, vol. 55, no. 8, pp. 1906–1912, 2016.

[14] T. Ishigure, H. Masuda, K. Date, C. Marushima, and T. Enomoto, "Direct fabrication for polymer optical waveguide in PMT ferrule using the Mosquito method," in *Proc. 68th Electron. Compon. Technol. Conf.*, 2018, pp. 1103–1108.

[15] K. Date, K. Fukagata, and T. Ishigure, "Core position alignment in polymer optical waveguides fabricated using the Mosquito method," *Opt. Express*, vol. 26, no. 12, pp. 15632–15641, 2018.

[16] D. Marcuse, "Loss analysis of single-mode fiber splices," *Bell Sys. Tech. J.*, vol. 56, no. 5, pp. 703–718, May–Jun. 1977.

[17] S. Yakabe, Y. Kobayashi, H. Matsui, Y. Saito, K. Manabe, and T. Ishigure, "Low-loss single-mode polymer optical waveguide with perfectly circular cores," *Opt. Express*.

Sho Yakabe was born in Kanagawa, Japan, in 1987. He received the B.S. degree in applied physics and physico-informatics, and the M.S. degree in integrated design engineering in 2010 and 2012, respectively, from Keio University, Yokohama, Japan, where he is currently working toward the Ph.D. degree in material design science. He joined Sumitomo Electric Industries Ltd., in 2012. His main research project is the development of next-generation multi-fiber optical connectors.

Hitomi Matsui was born in Tokyo, Japan, in 1995. She received the B.S. and M.S. degrees in integrated design engineering from Keio University, Tokyo, Japan, in 2018 and 2020, respectively. She joined Nippon Telegraph and Telephone East Corporation in 2020.

Yui Kobayashi was born in Tokyo, Japan, in 1996. She received the B.S. degree in applied physics and physico-informatics in 2019 from Keio University, Yokohama, Japan, where she is currently working toward the M.S. degree in material design science. Her current research interests is in polymer optical waveguide based spot-size converters.

Yuki Saito was born in Chiba, Japan, in 1992. She received the B.S. degree in applied physics and physico-informatics, and the M.S. degree in integrated design engineering from Keio University, Yokohama, Japan, in 2015 and 2017, respectively. In 2017, she joined Sumitomo Electric Industries Ltd., Yokohama, Japan, and since then she has been involved in the research and development of optical fibers and optical fiber components.

Ken Manabe was born in Hyogo, Japan, in 1981. He received the B.S. and M.S. degrees in precision science and technology from Osaka University, Osaka, Japan, in 2003 and 2005, respectively. He joined Sumitomo Electric Industries Ltd., in 2005. His main research is the computer aided engineering.

Takaaki Ishigure (Senior Member, IEEE) received the B.S. degree in applied chemistry and the M.S. and Ph.D. degrees in material science from Keio University, Yokohama, Japan, in 1991, 1993, and 1996, respectively. In 2005, he was with the Department of Electrical Engineering, Columbia University, New York, NY, USA, as a Visiting Research Scientist. He is currently a Professor with the Faculty of Science and Technology, Department of Applied-Physics and Physic-Informatics, Keio University. His current research interests are in on-board optical interconnections realized with multimode/single-mode polymer optical waveguides. He has authored or coauthored more than 60 original journal papers and 200 international conference papers including several invited papers. He works as a committee member of IEEE and SPIE conferences. He was the General Chair of the IEEE CPMT Symposium Japan (ICSJ2019). He and his group were awarded the Outstanding Session Paper Award in the 64th ECTC conference in 2015 and the Outstanding Poster Paper Award in the 61st ECTC conference in 2012.